



# Milestone progress of the HEPS booster commissioning

Yue-Mei Peng<sup>1,2</sup> · Jian-She Cao<sup>1</sup> · Jin-Hui Chen<sup>1</sup> · Hai-Yi Dong<sup>1</sup> · Ping He<sup>1</sup> · Yi Jiao<sup>1,2</sup> · Ling Kang<sup>1</sup> · Wen Kang<sup>1</sup> · Jian Li<sup>1</sup> · Jing-Yi Li<sup>1</sup> · Guo-Ping Lin<sup>1</sup> · Fang Liu<sup>1</sup> · Feng-Li Long<sup>1,2</sup> · Cai Meng<sup>1,2</sup> · Xin Qi<sup>1</sup> · Hua-Min Qu<sup>1</sup> · Yan-Feng Sui<sup>1,2</sup> · Sheng Wang<sup>1</sup> · Gang Xu<sup>1</sup> · Qiang Ye<sup>1</sup> · Jing Zhang<sup>1</sup> · Pei Zhang<sup>1</sup> · Wei-Min Pan<sup>1,2</sup>

Received: 25 November 2023 / Revised: 12 December 2023 / Accepted: 24 December 2023 / Published online: 1 February 2024  
© The Author(s), under exclusive licence to China Science Publishing & Media Ltd. (Science Press), Shanghai Institute of Applied Physics, the Chinese Academy of Sciences, Chinese Nuclear Society 2024

## Abstract

The high-energy photon source (HEPS) is the first fourth-generation synchrotron light source facility in China. The HEPS injector consists of a linear accelerator (Linac) and a full energy booster. The booster captures the electron beam from the Linac and increases its energy to the value required for the storage ring. The full-energy beam could be injected to the storage ring directly or after “high-energy accumulation.” On November 17, 2023, the key booster parameters successfully reached their corresponding target values. These milestone results were achieved based on numerous contributions, including nearly a decade of physical design, years of equipment development and installation, and months of beam commissioning. As measured at the extraction energy of 6 GeV, the averaged beam current and emittance reached 8.57 mA with 5 bunches and 30.37 nm rad with a single-bunch charge of 5.58 nC, compared with the corresponding target values of 6.6 mA and 35 nm rad, respectively. This paper presents the physical design, equipment development, installation, and commissioning process of the HEPS booster.

**Keywords** High energy photon source · Booster · Beam commissioning

## 1 Introduction

As the first fourth-generation synchrotron radiation light source in China, the high-energy photon source (HEPS) [1, 2] is under construction in Huairou Science City, Beijing, China. The HEPS complex consists of a 500-MeV linear accelerator (Linac) [3], a full energy booster [4], a 6-GeV

storage ring with a circumference of approximately 1.36 km [5], three transfer lines [6], and multiple beamlines and the corresponding experimental stations. The layout of the HEPS complex is illustrated in Fig. 1. Construction of the facility began in June 2019 with a scheduled construction period of 6.5 years. Once completed, the HEPS will be an important platform for supporting original and innovative research in the fields of basic and engineering sciences.

As a full-energy injector, the HEPS booster increases the energy of the electron beam from the Linac to a design energy of 6 GeV and provides a sufficiently high-quality electron beam for injection into the storage ring. Several milestones in booster technology have been achieved in the past few years. The physical design and component layout were finalized in December 2019. The pre-alignment installation of the magnet-vacuum units began in March 2022, and installation of the magnet units in the tunnel started in August of the same year. After installation and conditioning of the equipment were completed in the middle of 2023, beam commissioning began at the end of July 2023. In November 2023, an electron beam with a single-bunch charge of more than 5 nC was successfully ramped up to 6 GeV.

---

This work was supported by the National Natural Science Foundation of China (No. 12005239).

✉ Yi Jiao  
jiaoyi@ihep.ac.cn

✉ Jing-Yi Li  
jingyili@ihep.ac.cn

✉ Wei-Min Pan  
panwm@ihep.ac.cn

<sup>1</sup> Key Laboratory of Particle Acceleration Physics and Technology, Institute of High Energy Physics, Chinese Academy of Sciences, 19B Yuquan Road, Shijingshan District, Beijing 100049, China

<sup>2</sup> University of the Chinese Academy of Sciences, 19A Yuquan Road, Shijingshan District, Beijing 100049, China

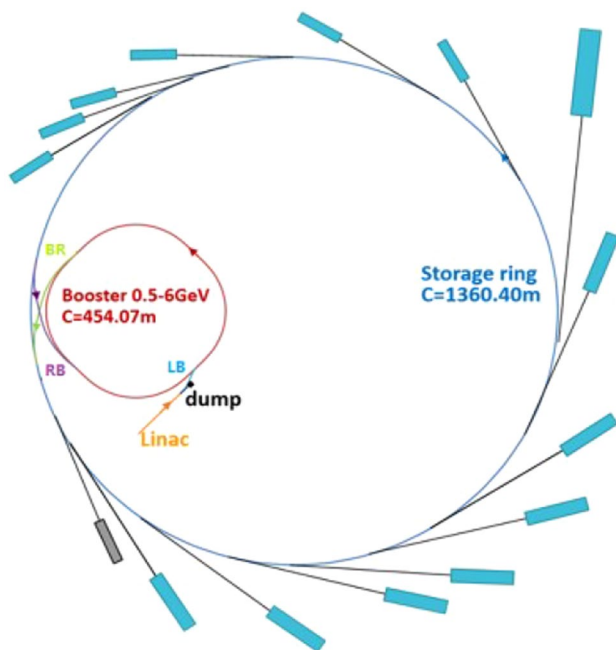


**Fig. 1** (Color online) Layout of the high-energy photon source (HEPS) complex. (LB is the transport line that connects the Linac and the booster, BR is the transport line that can transfer the beam from the booster to the storage ring, and RB is the transport line that can transfer the beam from the storage ring to the booster.)

The remainder of this paper is organized as follows. In Sect. 2, the selection of key parameters and the evolution of the booster lattice design are introduced. The engineering design, equipment installation, and conditioning are reviewed in Sect. 3, and the beam commissioning is described in Sect. 4. Finally, a brief summary is presented in the final section.

## 2 Physical design of the high-energy photon source (HEPS) booster

As a fourth-generation synchrotron light source, a multi-bend achromat lattice was adopted in the HEPS storage ring to achieve an ultralow emittance, a natural emittance below  $60 \text{ pm}\cdot\text{rad}$ , and high brightness of up to  $1 \times 10^{22} \text{ phs/s/mm}^2/\text{mrad}^2/0.1\% \text{ BW}$ . However, this ultralow-emittance design introduced a series of physical and technical challenges, which were reflected in the design of the HEPS booster.

First, the booster should provide electron bunches with a bunch charge of up to  $5 \text{ nC}$ . Owing to the small dynamic acceptance of the storage ring, an on-axis swap-out injection [7] was selected as the baseline scheme, which, however, required the booster to provide bunches with sufficiently high charge during each injection process. In this scenario, the maximum charge per bunch was approximately  $14.4 \text{ nC}$ .

To reduce the requirement for the charge per bunch injected into the booster at  $500 \text{ MeV}$ , the so-called “high-energy accumulation” scheme [8] was proposed.

The implementation of the “high-energy accumulation” scheme required adding a high-energy transport line that could transfer the beam from the storage ring to the booster and a high-energy injection system to support off-axis injection in the booster. When the storage ring is refilled with the electron beam, the bunch with the lowest charge is extracted and injected into the booster. This bunch then merges with an existing bunch in the booster that has been injected from the Linac and is accelerated to  $6 \text{ GeV}$ . After more than three damping cycles, the merged bunch is extracted from the booster and reinjected into the storage ring. In this scheme, the booster is used as the accumulator at  $6 \text{ GeV}$ .

Nevertheless, the charge per bunch injected into the booster at  $500 \text{ MeV}$  must still be not less than  $2.5 \text{ nC}$ . Considering difficulties in the initial commissioning of the storage ring, the charge-per-bunch injected into the booster at  $500 \text{ MeV}$  and ramped to  $6 \text{ GeV}$  were increased to  $6.25$  and  $5 \text{ nC}$ , respectively, which means that a transmission efficiency of  $80\%$  during the ramping process is required. Such a high bunch charge brings challenges to both the booster and the Linac.

Because on-axis injection was adopted for the booster at  $500 \text{ MeV}$ , the Linac must provide an electron pulse with a charge of not less than  $6.25 \text{ nC}$ . Considering weak radiation damping and collective instabilities at  $500 \text{ MeV}$ , various studies have been conducted to investigate the bunch charge threshold at this energy. These studies indicate [9–12] that the transverse mode coupling instability (TMCI) threshold is a key factor limiting the charge per bunch at low energies, and increasing the momentum compaction factor is an effective way to increase the TMCI threshold. Consequently, the FODO cell was selected as the basic lattice structure [4]. With such a simple and reliable structure, a relatively large momentum compaction factor of approximately  $3.7 \times 10^{-3}$  was achieved in the design, yielding a sufficiently high bunch charge threshold.

In addition, for mitigating the impact of the booster operation on beam orbit fluctuations in the storage ring and simultaneously implementing beam commissioning of the booster and tunnel installation of the storage ring, it was decided to locate the booster in a separate tunnel with a circumference of approximately one-third of that of the storage ring.

After several years of evolution, the booster lattice was finalized at the end of 2019. The lattice has four super-periods. Each super-period consists of 14 standard FODO cells and matching sections at both ends, containing 32 dipole magnets, 37 quadrupole magnets, and 17 sextupole magnets. Each period provided a dispersion-free straight section of approximately  $8.8 \text{ m}$  for the low-energy injection,

extraction, high-energy injection, and RF system equipment. The Lambertson-type septum magnets was adopted in the HEPS booster design to maintain the tunnel of the Linac, booster, and storage ring on the same horizontal plane, whereas the injection and extraction of the booster occur in the vertical plane. In the high-energy injection design, a dedicated  $\pi$ -section was designed, with two kickers placed at both ends to form a local bump. Compared to the conventional 4-kicker injection scheme, this scheme reduces the number of kickers as well as the impedance budget and cost. Additionally, in the high-energy extraction design, four fast bumper magnets [13] were placed to form a local bump and reduce the required kicker strength. The layout and optics of one super-period in the HEPS booster are shown in Fig. 2.

Studies on the transmission efficiency during injection and ramping [14], fringe field effects [15], eddy current effects during the ramping process [16], and error effects on beam dynamics [17] have also been performed to ensure that there are no showstoppers in the beam dynamics point of view. Some key booster parameters are listed in Table 1.

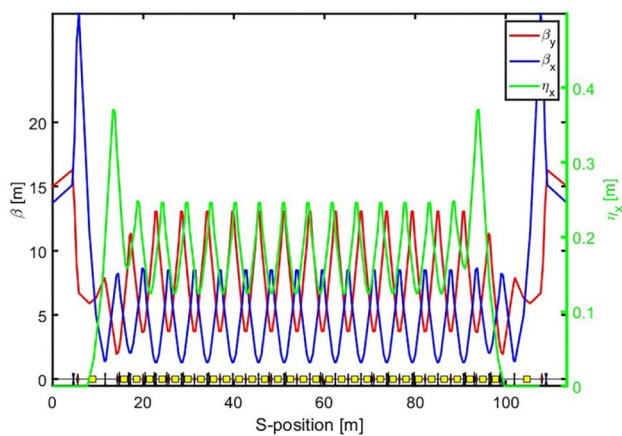


**Fig. 2** (Color online) Layout and optics of a super-period in the booster

### 3 Equipment development and commissioning preparation

To build a high-performance full-energy injector, the booster was designed considering both robustness and advancement. After iterative optimization, the technical designs of the accelerator physics and equipment were finalized by the end of 2019 [13, 18–24].

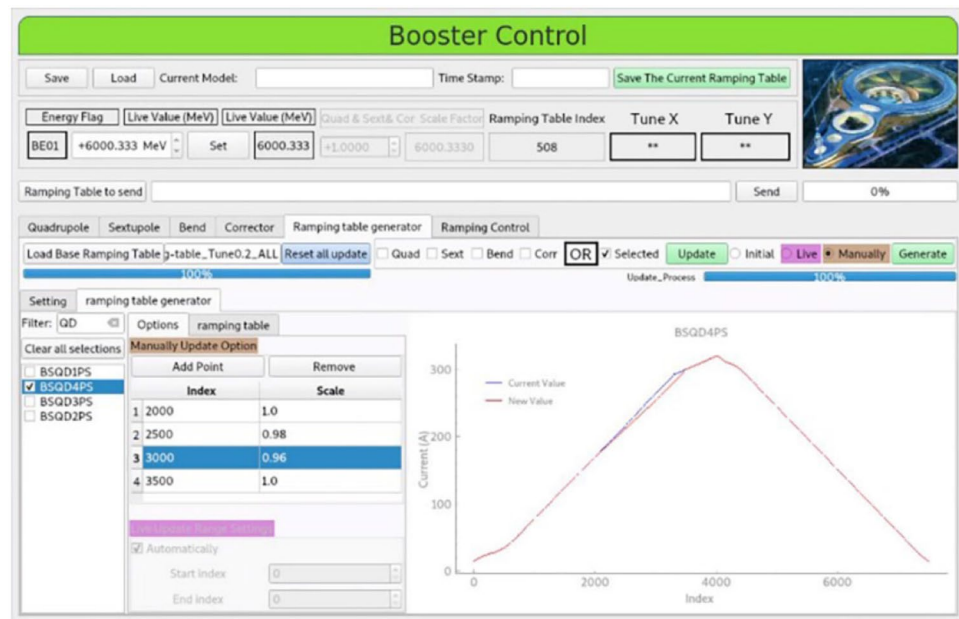
Four main types of magnets were installed in the booster: dipoles, quadrupoles, sextupoles, and orbit correctors. The iron cores of these magnets were made of 0.55-mm thick silicon–steel laminations to mitigate the eddy current effect during energy ramping. All these magnets were carefully sorted to minimize field uniformity-induced effects [25]. The magnets of each type (excluding the orbit correctors) were grouped into several families. The dipoles in each arc were set as a family, and four groups of dipoles were established. The quadrupoles were divided into eight families, and the sextupoles were grouped into six families. Each family of magnets was connected in series and energized using the same power supply (PS). All of these PSs were synchronized during the ramping up and down processes. The ramping processes were guided by a pre-generated table. The ramping table was produced according to the I-BL curve determined by the magnetic field measurements. The ramping process can be programmed to stop and remain at any energy between the injection and extraction energies and work as a storage ring. This feature enables researchers to conduct energy-dependent machine studies and ramp curve optimization. This is shown in Fig. 3. The beam energy stays at 6 GeV. The strength of QD4 was optimized to adjust the tune and, based on the optimized strength, the ramping curve was updated online. Using the controllers developed in-house, the magnet PSs have been working reliably, with both small dynamic tracking errors and high stability in the DC mode.

The vacuum chamber of the booster was mainly made of stainless steel type 316 L to achieve a permeability of less than 1.02 after manufacturing. The adopted thickness

**Table 1** Key parameters of the HEPS booster

Parameters	Design value	Target value	Measured value
Energy (MeV)	500–6000	500–6000	$6001.20 \pm 0.30$
Repetition rate (Hz)	1	~1	1.07
Max. beam current @ 500 MeV (mA)	11 @ 10 bunches	8.25 @ 5 bunches	Avg. value: 8.951 Max. value: 11.489
Max. beam current @ 6 GeV (mA)	13 (w/high energy accumulation)	6.6 @ 5 bunches	Avg. value: 8.571 Max. value: 9.367
Bunch charge @ 6 GeV (nC)	$\geq 2$	$\geq 5$	Avg. value: 5.409 Max. value: 5.650
Natural emittance @ 6 GeV (nm)	35	$\leq 35$	$30.37 \pm 0.30$ @ $5.58 \pm 0.05$ nC
Energy spread @ 6 GeV (%)	0.096	~0.1	$0.0994 \pm 0.0029$ @ $5.58 \pm 0.05$ nC

**Fig. 3** (Color online) Interface of the HEPS booster control application



of the chambers was 0.7 mm to reduce the eddy current induced by the varying magnetic field during energy ramping. Because the booster was designed as a charge accumulator at 6 GeV, the maximum average beam current is higher than 13 mA. In this scenario, the estimated heat load produced by synchrotron radiation can exceed 290 W/m. Water-cooling of the vacuum chambers was adopted to avoid deformation and protect critical equipment.

The booster was equipped with six PETRA-type 5-cell normal conducting RF cavities working at 499.8 MHz. Only five of them were installed at the current stage, leaving the other for offline testing. They will likely be used by the storage ring during vacuum cleaning. The RF voltage and phase were ramped with magnet PSs. Because of the lack of high-order mode (HOM) dampers, this type of cavity is suspected to be rich in HOMs when operating with a beam. Previous studies [26] indicated that the growth time of coupled-bunch instabilities driven by dangerous HOMs is short. The planned curing method included adjusting the temperature of the cooling water and the resonant frequencies of the cavities. A bunch-by-bunch feedback system is also planned.

Lambertson-type septum magnets are used to guide the electron beam entering the booster from the transport line during injections and vice versa during extraction. Slotted-pipe kickers driven by LC series resonant pulsed PSs are employed to kick the electron beam into the booster acceptance when injecting and exiting the booster for extraction. The pulse length of the kickers allows the filling of five evenly distributed buckets or any combination of these five buckets in the booster ring.

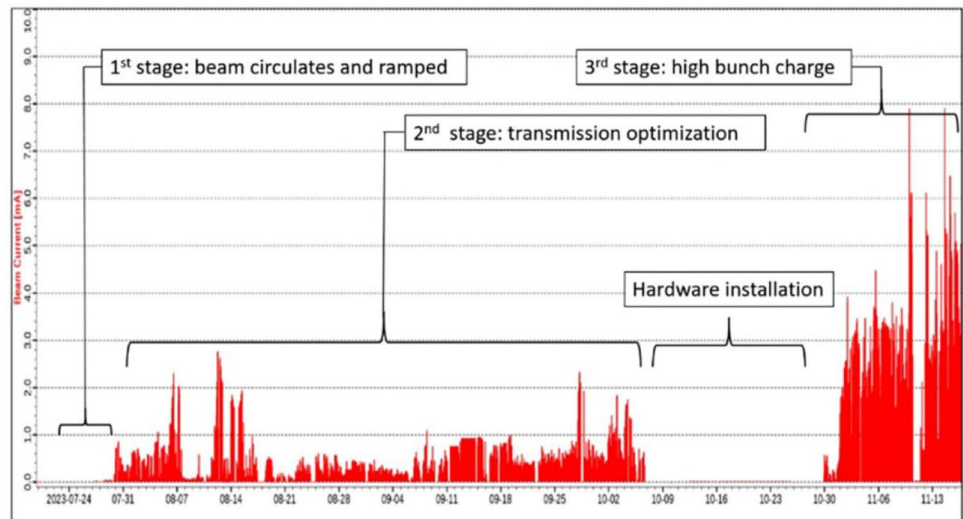
An equipment installation experiment was conducted prior to magnet-unit pre-alignment and installation in the tunnel to verify the layout design. Installation procedures, wiring, and water-cooling arrangements and connections were optimized and finalized with the aid of this experiment. The vast installation of pre-aligned magnetic units, which started approximately five months earlier, was launched in August 2022. After approximately five months of installation, and six months of wiring and equipment testing, the booster was ready to be commissioned in July 2023.

The HEPS physics team has developed a rich set of high-level applications (HLAs). All these HLAs are based on the independently developed application framework *Pyapas* [27]. Owing to their modular design, principle based on physical quantities, and ability to run simulation models online from *Pyapas*, the development efficiency and reliability of the HLAs have been greatly improved. These features of HLAs allow researchers to control the beams more intuitively.

## 4 Beam commissioning

The beam commissioning of the booster began on July 25, 2023. As illustrated in Fig. 4, the commissioning process was divided into three stages. In the first two weeks, efforts were made to circulate the beam in the booster ring and capture it using RF buckets. In this stage, we observed the beam injection through the beam position monitor (BPM) row data. Twenty turns were performed by scanning the kicker strength and fine-tuning the corrector strength near

**Fig. 4** Historical curve of beam current during the booster commissioning process



the injection point. After adjusting the set of injection energies in the booster, the beam remained for more than 25 ms. Based on the theoretical response matrix and turn-by-turn (TBT) data, the orbit was preliminarily corrected. Subsequently, the sextupole magnets were powered on, the RF cavities were turned on, and beam accumulation was achieved after RF frequency correction. The beam energy was also ramped up to 6 GeV during this stage.

The following stage, which took approximately 2 months, was mainly focused on optimizing the beam transmission efficiency during the injection and ramping processes. The equipment performance also improved in this stage. A bunch charge of less than 3 nC from the Linac was used to reduce the radiation dose. A total transmission efficiency greater than 80% were achieved with this configuration in late September. To improve the transmission efficiency, the beam dynamics were optimized for both the injection and ramping processes. In addition to optimizing the energy, position, angle, and distribution of the injected beam, the RF voltage and phase were adjusted, the delay time of the PSs was optimized, the closed orbit was corrected, and tuning was performed. During the ramping process at this stage, each RF cavity must provide a voltage greater than 1.6 MV, and the power used was almost at its limit. This made it prone to vacuum protection or open loops, thus imposing several restrictions on energy-ramping operations.

In the third commissioning stage, approximately 20 days after equipment installation, a high bunch charge was mainly pursued. The Linac was tuned to provide  $> 8$  nC at the exit. When the Twiss parameters were matched at both ends of the low-energy transport line based on the beam parameter at its entrance, the bunch charge increased to more than 6.5 nC at the end of the transport line. Owing to these efforts, a bunch charge of more than 5 nC was ramped up to 6 GeV on November 6, 2023. Since then, multi-bunch mode

commissioning and repetition rate improvements have been performed. By November 17, all the target values proposed in the preliminary design report were reached. The results are summarized in Table 1. In the table, the beam energy is directly calibrated by the dipole strength (I-BL), emittance, and energy spread directly given by the synchrotron light monitor, as well as the beam current and bunch charge provided by the DCCT and BCM. When measuring the beam current and bunch charge, we conducted 11 measurements and obtained statistical values. When measuring the repetition rate, we calculated the number of cycles completed in 0.5 min. The value of 1.07 Hz is the highest value achieved thus far, and a repetition rate below 1.07 Hz is acceptable. These results indicate that the booster qualifies for subsequent commissioning of the storage ring. As the storage ring is still in equipment installation phase, the “high-energy accumulation” scheme was not tested in this period of commissioning. It is worth mentioning that the coupled-bunch instabilities driven by dangerous HOMs did not occur during the beam commissioning process, and the bunch-by-bunch feedback system has not yet started working.

During the commissioning, the most challenging goal was to achieve a single-bunch charge above 5 nC at 6 GeV. In response to this challenge, efforts have been made to improve the transmission efficiency of the entire process and increase the pulse charge from the Linac. To improve transmission efficiency, the beam dynamics were optimized both horizontally and longitudinally. Considering the horizontal factors, the entrance angle, position, and distribution of the injection beam were scanned to obtain optimal values. The orbit and optical errors of the booster were adjusted to increase the capture and ramping transmission rates. Beam loss mainly occurred below 1 GeV, and many efforts have been made at these energy points, such as tuning, and the closed orbit was optimized to a stable region, as shown in

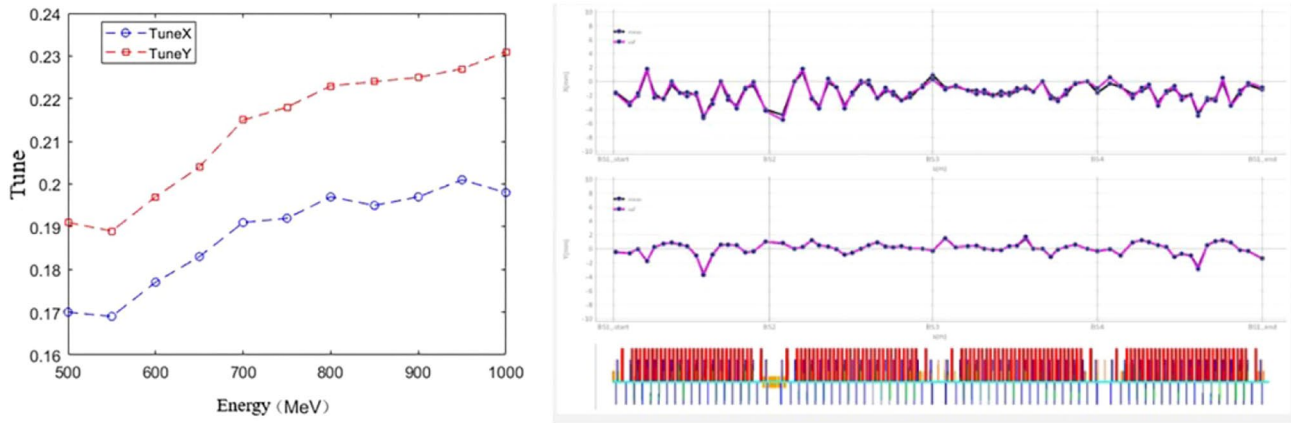


**Fig. 5** (Color online) Tune (left) and closed orbit (right) in the HEPS booster

Fig. 5. We also optimized the optics by using the theoretically designed lattice as the target at 6 GeV. After correction, beta-beating was approximately 2% (RMS) in both the horizontal and vertical planes (Fig. 6).

On the longitudinal side, the energy of the injection beam was carefully matched to that of the booster by adjusting the injection energy settings of the booster. The voltage and phase of the RF cavities are other longitudinal factors that affect efficiency. These parameters were tuned to achieve the best capture. The total transmission efficiency reached over 80%, which was calculated using the amount of charge at the end of the transport line and when the booster was ramped to 6 GeV.

Finally, with a sufficient pulse charge from the Linac, a single-bunch charge of over 5 nC at 6 GeV was successfully

achieved. Figure 7 shows a typical charge transmission in an injection-ramping cycle.

## 5 Summary

After nearly a decade of physics design, years of equipment development and installation, and months of beam commissioning, the HEPS booster has recently reached the commissioning goal of a bunch charge of over 5 nC at 6 GeV. This validates the physical design and demonstrates that the equipment performance meets the design requirements. The beam parameters of the HEPS booster can satisfy the requirements for the subsequent commissioning of the storage ring. Improvement in performance of the booster

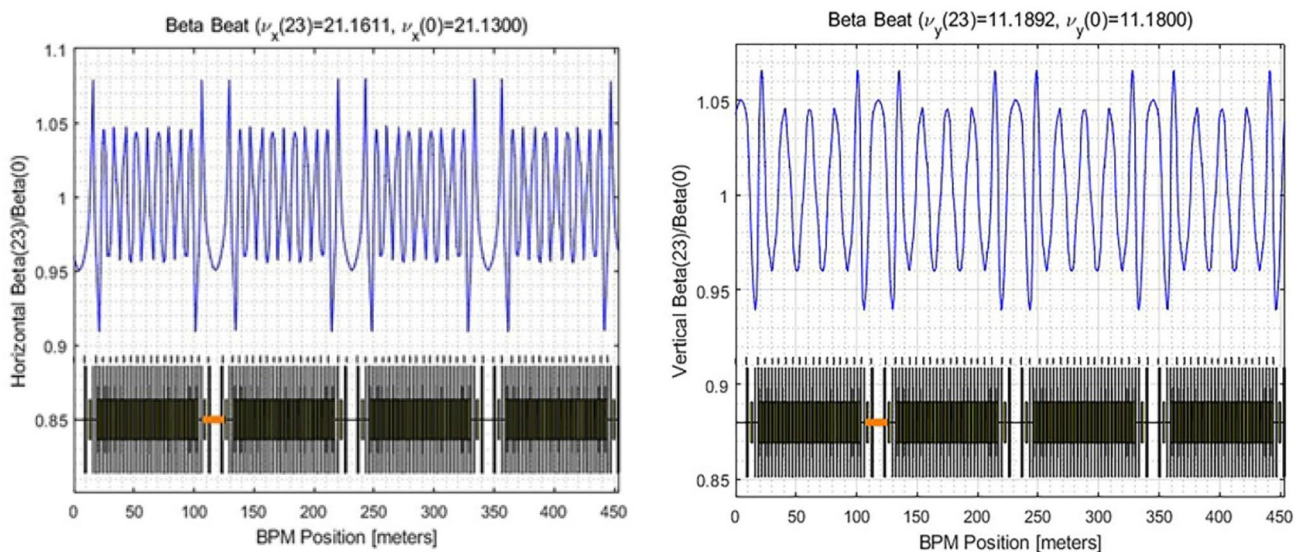
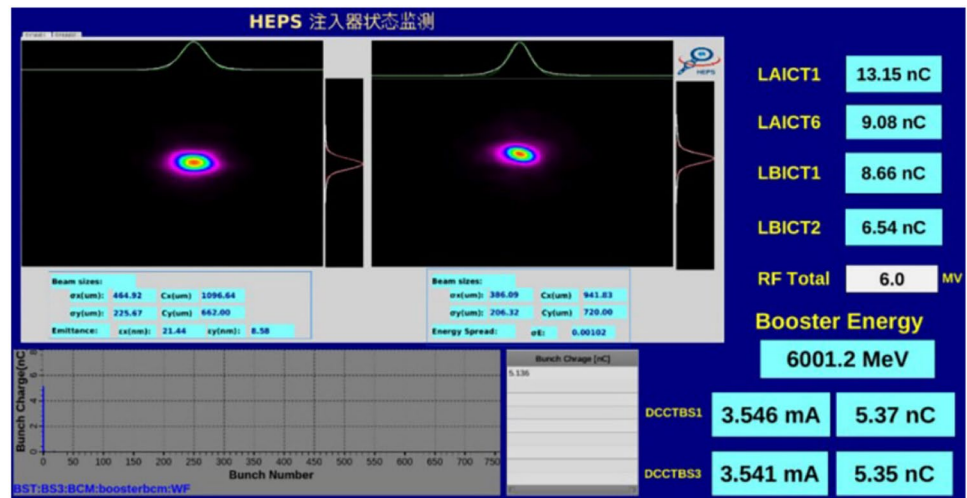


**Fig. 6** (Color online) Beta-beating in the HEPS booster at 6 GeV

**Fig. 7** (Color online) Screenshot of beam status monitoring. (LAICT1 is the ICT downstream of the electron gun, LBICT1 is an ICT at the entrance of the transport line LB, LBICT2 is an ICT at the end of the transport line LB, “RF total” means the total RF voltage in the booster, DCCTBS1 and DCCTBS3 are two DCCTs in the booster.)



will continue. Besides serving as a full energy injector, the HEPS booster can be operated as a storage ring at any energy between 0.5 and 6 GeV for beam physics experiments of interest.

**Acknowledgements** The authors thank all those involved in the design, construction, and commissioning of the HEPS booster.

**Author contributions** All authors contributed to the study conception and design. Material preparation, data collection, and analysis were performed by Y-MP, J-YL, and YJ. The first draft of the manuscript was written by Y-MP, and all authors commented on previous versions of the manuscript. All authors read and approved the final manuscript.

**Data availability** The data that support the findings of this study are openly available in Science Data Bank at <https://cstr.cn/31253.11.scien.cedb.j00186.00370> and <https://doi.org/https://doi.org/10.57760/scien.cedb.j00186.00370>.

**Conflict of interest** Yi Jiao is an editorial board member for Nuclear Science and Techniques and was not involved in the editorial review, or the decision to publish this article. All authors declare that there are no competing interests.

## References

1. Y. Jiao, G. Xu, X.H. Cui et al., The HEPS project. *J. Synchrotron Rad.* **25**(6), 1611–1618 (2018). <https://doi.org/10.1107/s1600577518012110>
2. Y. Jiao, W.M. Pan, High energy photon source. *High Power Laser Part. Beams* **34**, 104002 (2022). <https://doi.org/10.11884/HPLPB202234.220080>
3. C. Meng, X. He, X.J. Nie et al., Physics design of the HEPS Linac. *Radiat. Detect. Technol. Methods* **4**, 497–506 (2020). <https://doi.org/10.1007/s41605-020-00205-w>
4. Y.M. Peng, Z. Duan, Y.Y. Guo et al., Design of the HEPS booster lattice. *Radiat. Detect. Technol. Methods* **4**, 425–432 (2020). <https://doi.org/10.1007/s41605-020-00202-z>
5. Y. Jiao, F.S. Chen, P. He et al., Modification and optimization of the storage ring lattice of the High Energy Photon Source. *Radiat. Detect. Technol. Methods* **4**, 415–424 (2020). <https://doi.org/10.1007/s41605-020-00189-7>
6. Y.Y. Guo, Y.Y. Wei, Y.M. Peng et al., The transfer line design for the HEPS project. *Radiat. Detect. Technol. Methods* **4**, 440–447 (2020). <https://doi.org/10.1007/s41605-020-00209-6>
7. Z. Duan, J.H. Chen, Y.Y. Guo et al., The swap-out injection scheme for the High Energy Photon Source, in *Proc of IPAC'18, Vancouver, Canada, 2018* (2018), pp. 4178–4181
8. Y.M. Peng, Z. Duan, Y.Y. Guo et al., Status of HEPS booster lattice design and physics studies, in *Proc of IPAC'18, Vancouver, Canada* (2018), pp. 1407–1410
9. Y.M. Peng, J.Y. Li, C. Meng et al., The considerations of improving TMCI threshold on HEPS booster, in *Proc of IPAC'18, Vancouver, Canada* (2018), pp. 1411–1413
10. H.S. Xu, N. Wang, The influence of chromaticity on transverse single-bunch instability in the booster of HEPS, in *Proc of IPAC'18, Vancouver, Canada* (2018), pp. 2968–2970
11. H.S. Xu, Z. Duan, J.Y. Li et al., Studies of the single-bunch instabilities in the booster of HEPS, in *Proc of IPAC'18, Vancouver, Canada* (2018), pp. 2971–2974
12. H.S. Xu, Y.M. Peng, N. Wang, The study of single-bunch instabilities in the ramping process in the HEPS booster, in *Proc of IPAC'19, Melbourne, Australia* (2019), pp. 206–209
13. L.H. Huo, J.H. Chen, G.W. Wang et al., Development of the pulse bump magnet in HEPS. *Radiat. Detect. Technol. Methods* **7**, 521–530 (2023). <https://doi.org/10.1007/s41605-023-00419-8>
14. Y.M. Peng, Z. Duan, C. Meng et al., Study of beam transmission efficiency in injection and ramping process of the HEPS booster, in *Proc of IPAC'21, Campinas, SP, Brazil* (2021), pp. 225–228
15. Y.Y. Guo, N. Li, Y.M. Peng et al., Study on the fringe field effects in HEPS booster. *Radiat. Detect. Technol. Methods* **7**, 382–386 (2023). <https://doi.org/10.1007/s41605-023-00407-y>
16. Y.M. Peng, J.Y. Li, C. Meng et al., Study of the ramping process for HEPS booster, in *Proc of IPAC'19, Melbourne, Australia* (2019), pp. 1521–1523
17. C. Meng, D.H. Ji, J.Y. Li et al., Error study of HEPS booster, in *Proc of IPAC'18, Vancouver, Canada* (2018), pp. 1398–1400
18. W. Kang, L. Liu, Y.J. Yu et al., Design of the magnets for the HEPS injector. *Radiat. Detect. Technol. Methods* **6**, 143–149 (2022). <https://doi.org/10.1007/s41605-022-00314-8>
19. Y.L. Luo, J. Li, P. Zhang et al., Development of a 500-MHz waveguide directional coupler with high directivity for HEPS. *Radiat. Detect. Technol. Methods* **6**, 323–329 (2022). <https://doi.org/10.1007/s41605-022-00323-7>

20. P. Zhang, J.P. Dai, Z.W. Deng et al., Radio-frequency system of the high energy photon source. *Radiat. Detect. Technol. Methods* **7**, 159–170 (2023). <https://doi.org/10.1007/s41605-022-00366-w>
21. C. Han, F.L. Long, Y. Gao et al., Development of corrector magnet power supply for high energy photon source. *Radiat. Detect. Technol. Methods* **6**, 470–478 (2022). <https://doi.org/10.1007/s41605-022-00346-0>
22. X.L. Guo, F.L. Long, C. Han et al., Design of digital controller for HEPS corrector power supply. *Radiat. Detect. Technol. Methods* **7**, 387–391 (2023). <https://doi.org/10.1007/s41605-023-00404-1>
23. J. He, Y.F. Sui, Y. Li et al., Beam position monitor design for the High Energy Photon Source. *Meas. Sci. Technol.* **33**, 115106 (2022). <https://doi.org/10.1088/1361-6501/ac8277>
24. J. He, Y.F. Sui, Y. Li et al., Beam position monitor characterization for the High Energy Photon Source Synchrotron. *Symmetry* **15**, 660 (2023). <https://doi.org/10.3390/sym15030660>
25. Y.M. Peng, J.X. Zhou, J.T. Pan, Study of magnets sorting for the HEPS booster, in *Proc of IPAC'23, Venice, Italy* (2023), pp. 1088–1090
26. H.S. Xu, P.F. Liang, Y.M. Peng et al., Studies of coupled-bunch instabilities in the HEPS booster, in *Proc of IPAC'23, Venice, Italy* (2023), pp. 3566–3569
27. X.H. Lu, Q. Ye, H.F. Ji et al., Status of high-level application development for HEPS, in *Proc of ICALEPCS2021, Shanghai, China* (2021), pp. 978–980

Springer Nature or its licensor (e.g. a society or other partner) holds exclusive rights to this article under a publishing agreement with the author(s) or other rightsholder(s); author self-archiving of the accepted manuscript version of this article is solely governed by the terms of such publishing agreement and applicable law.